

Transport properties of disordered carbon nanotubes with long-range Coulomb interaction

Hideo Yoshioka

Department of Physics, Nagoya University, Nagoya 464-8602, Japan

and Department of Applied Physics, Delft University of Technology, Lorentzweg 1, 2628 CJ Delft, The Netherlands

(Received 26 March 1999; revised manuscript received 16 December 1999)

Transport properties of disordered carbon nanotubes are investigated including long-range Coulomb interaction. The resistivity and optical conductivity are calculated by using the memory functional method. In addition, the effect of localization is taken into account by use of the renormalization-group analysis, and it is shown that the backward scattering of the intravalley and that of the intervalley cannot coexist in the localized regime. Differences between the transport properties for the metallic state with two valleys and those with one valley are discussed.

Single wall carbon nanotubes (SWNT's) are the new materials that are an experimental realization of one-dimensional (1D) electron systems.¹ Since the SWNT is made by rolling up a graphite sheet, it is expected that fascinating properties different from the conventional quantum wires made from semiconductor heterostructures will be observed. From this point of view, transport properties of disordered SWNT's have been discussed in Refs. 2 and 3. It has been predicted that the backward scattering due to the impurities vanishes when the range of the impurity potential is much larger than the lattice constant, but that the backward scattering reappears when applying a magnetic field perpendicular to the tube axis. It should be noted that the absence of the backward scattering holds for the graphite sheet as well as any SWNT's.

In the above studies, electron correlations have been neglected. The 1D nature together with the electron-electron interaction has been known to result in a variety of correlation effects in SWNT's in case of short range interactions⁴⁻⁶ and of the long-range Coulomb interaction.⁷⁻¹⁰ Effects of electronic correlation in SWNT's have been measured in the Coulomb blockade regime¹¹ as well as for Ohmic contacts.¹² In the latter experiment, power-law dependences of the conductance as a function of temperature and of the differential conductance as a function of bias voltage have been observed and interpreted in terms of tunneling into clean SWNT with the interaction.

Even when the Coulomb interaction is taken into account, the conclusion of the absence of the backward scattering in Refs. 2 and 3 is not changed. However, the effects of the Coulomb interaction on the transport in disordered SWNT's should be observable in case of shorter range impurity potentials. In the present paper, I will discuss the transport properties of SWNT's with short range impurity potentials and the long-range Coulomb interaction. It is shown that the interaction gives rise to an enhanced resistivity compared to that without the interaction. In addition, the interaction leads to a power-law dependence of the resistivity as a function of temperature and modifies the power of the frequency for the optical conductivity. In the localized regime, it is found that intravalley and intervalley backward scattering cannot coexist.

The SWNT has metallic bands when the wrapping vector, $\vec{w} = N_+ \vec{a}_+ + N_- \vec{a}_-$, satisfies the condition, $N_+ - N_- = 0$

mod 3, where $\vec{a}_\pm = (\pm 1, \sqrt{3})a/2$ with a being the lattice constant. The Hamiltonian of the metallic SWNT with the long-range Coulomb interaction is written by the slowly varying Fermi field, ψ_{pas} , of the sublattice $p = \pm$, the spin $s = \pm$ and the valley $\alpha = \pm$, as follows:¹⁰

$$\mathcal{H}_0 = -iv_0 \sum_{pas} \alpha e^{-ip\alpha\chi} \int dx \psi_{pas}^\dagger \partial_x \psi_{-pas} + \frac{\bar{V}(0)}{2} \int dx \rho(x)^2, \quad (1)$$

where $\rho(x) = \sum_{pas} \psi_{pas}^\dagger \psi_{pas}$, $v_0 \approx 8 \times 10^5$ m/s, and $\bar{V}(0) = 2e^2/\kappa \ln(R_s/R)$ with $\kappa \approx 1.4$, R_s and R being the cutoff of long range of the Coulomb interaction and the radius of the tube, respectively. In Eq. (1), $\chi = \tan^{-1}[(N_+ - N_-)/\sqrt{3}(N_+ + N_-)]$ is the chiral angle ($\chi = 0$ corresponds to an armchair nanotube). In the above expression, I disregard the matrix elements of the interaction of the order of a/R , which lead to energy gaps.⁷⁻¹⁰ Therefore, the present theory is valid when the temperature T , or the frequency ω , are larger than the gaps induced by the Coulomb interaction.

The impurity potential introduced as disorder of the atomic potential is given by the following Hamiltonian,² $\mathcal{H}_{imp} = \sum_{p\alpha\alpha'} \int dx V_{\alpha\alpha'}^p(x) \psi_{pas}^\dagger \psi_{p\alpha's}$, where $V_{\alpha\alpha'}^p(x)$ is the impurity potential at the sublattice, p , by which the electron on the valley, α' , is scattered into the valley, α .¹³ Here I diagonalize the kinetic term in Eq. (1) and move to the basis of the right-moving ($r = +$) and the left-moving ($r = -$) electrons by the unitary transformation, $\psi_{pas} = (e^{-ip\alpha\chi/2}/\sqrt{2}) \sum_r (\alpha r)^{(1-p)/2} \psi_{ras}$. Then, \mathcal{H}_{imp} is written as follows:

$$\begin{aligned} \mathcal{H}_{imp} = \sum_{ras} \frac{1}{2} \int dx \{ & [V_{\alpha\alpha}^+(x) + V_{\alpha\alpha}^-(x)] \psi_{ras}^\dagger \psi_{ras} \\ & + [e^{i\alpha\chi} V_{\alpha-\alpha}^+(x) - e^{-i\alpha\chi} V_{\alpha-\alpha}^-(x)] \psi_{ras}^\dagger \psi_{r-\alpha s} \\ & + [V_{\alpha\alpha}^+(x) - V_{\alpha\alpha}^-(x)] \psi_{ras}^\dagger \psi_{-ras} + [e^{i\alpha\chi} V_{\alpha-\alpha}^+(x) \\ & + e^{-i\alpha\chi} V_{\alpha-\alpha}^-(x)] \psi_{ras}^\dagger \psi_{-r-\alpha s} \}. \end{aligned} \quad (2)$$

Here, the first (second) term expresses the intravalley (intervalley) forward scattering, and the third (fourth) one is the

intravalley (intervalley) backward scattering. When the range of the impurity potential is much larger than the lattice constant, $V_{\alpha\alpha}^+ = V_{\alpha\alpha}^-$ and $V_{\alpha-\alpha}^+ = V_{\alpha-\alpha}^- = 0$, which leads to vanishing of the third and fourth terms in Eq. (2), i.e., the absence of backward scattering, in agreement with Ref. 2. Here, I consider the case of an impurity potential with range shorter than the lattice constant by retaining finite matrix elements of the backward scattering in Eq. (2). I disregard forward scattering because it does not contribute to transport.

As was pointed out by Abrikosov and Ryzhkin,¹⁴ in 1D systems and in the limit of weak impurity potentials, the interaction between the electrons and the impurities can be parameterized by uncorrelated Gaussian random fields. Here, I extend this method to the present model and introduce two kinds of the random fields, $\eta(x)$ and $\xi(x)$, expressing the intravalley and the intervalley backward scattering, respectively. The fields have the probability distributions, $P_\eta = \exp\{-(2D_1)^{-1} \int dx \eta^2(x)\}$ and $P_\xi = \exp\{-(D_2)^{-1} \int dx \xi(x) \xi^*(x)\}$ where D_1 and D_2 are given by v_0/τ_1 and v_0/τ_2 with τ_1 (τ_2) being the scattering time due to the intravalley (intervalley) backward scattering. The Hamiltonian of the impurity potential is given by

$$\mathcal{H}_{imp} = \int dx \eta(x) \sum_{r\alpha s} \psi_{r\alpha s}^\dagger \psi_{-r\alpha s} + \int dx \left\{ \xi(x) \sum_{rs} \psi_{r+s}^\dagger \psi_{-r-s} + \text{H.c.} \right\}. \quad (3)$$

Note that the intravalley (intervalley) backward scattering, where the momentum transfer in the scattering process is small (large), is parameterized by a real (complex) field.

Here, I utilize the bosonization method and introduce the phase variables expressing the symmetric ($\delta = +$) and anti-symmetric ($\delta = -$) modes of the charge ($j = \rho$) and spin ($j = \sigma$) excitations, $\theta_{j\delta}$ and $\phi_{j\delta}$. The phase fields satisfy the commutation relation, $[\theta_{j\delta}(x), \phi_{j'\delta'}(x')] = i(\pi/2) \text{sign}(x - x') \delta_{jj'} \delta_{\delta\delta'}$. The Fermi field, $\psi_{r\alpha s}$, is expressed as

$$\psi_{r\alpha s} = \frac{\eta_{r\alpha s}}{\sqrt{2\pi\tilde{a}}} \exp \left[irq_F x + \frac{ir}{2} \{ \theta_{\alpha s} + r\phi_{\alpha s} \} \right], \quad (4)$$

where $\theta_{\alpha s} = \theta_{\rho+} + s\theta_{\sigma+} + \alpha\theta_{\rho-} + \alpha s\theta_{\sigma-}$, $\phi_{\alpha s} = \phi_{\rho+} + s\phi_{\sigma+} + \alpha\phi_{\rho-} + \alpha s\phi_{\sigma-}$, and \tilde{a}^{-1} is a large momentum cutoff.¹⁵ Klein factors $\eta_{r\alpha s}$ are introduced to ensure correct anticommutation rules for different species r, α, s , and satisfy $[\eta_{r\alpha s}, \eta_{r'\alpha's'}]_+ = 2\delta_{rr'}\delta_{\alpha\alpha'}\delta_{ss'}$. The spin-conserving products $\eta_{r\alpha s}\eta_{r'\alpha's'}$ in the Hamiltonian can be represented as,⁷ $A_{++}(r, \alpha, s) = \eta_{r\alpha s}\eta_{r\alpha s} = 1$, $A_{+-}(r, \alpha, s) = \eta_{r\alpha s}\eta_{r-\alpha s} = i\alpha\sigma_x$, $A_{-+}(r, \alpha, s) = \eta_{r\alpha s}\eta_{-r\alpha s} = ir\sigma_z$, and $A_{--}(r, \alpha, s) = \eta_{r\alpha s}\eta_{-r-\alpha s} = -ir\sigma_y$ with the standard Pauli matrices σ_i ($i = x, y, z$). The quantity $q_F = \pi n/4$ is related to the deviation n of the average electron density from half filling and can be controlled by the gate voltage. The Hamiltonian, \mathcal{H}_0 and $\mathcal{H}_{imp} = \sum_{i=1,2} \mathcal{H}_{imp}^i$, is expressed by the phase variables as follows:

$$\mathcal{H}_0 = \sum_{j=\rho,\sigma} \sum_{\delta=\pm} \frac{v_{j\delta}}{2\pi} \int dx \{ K_{j\delta}^{-1} (\partial_x \theta_{j\delta})^2 + K_{j\delta} (\partial_x \phi_{j\delta})^2 \}, \quad (5)$$

$$\mathcal{H}_{imp}^1 = \frac{i\sigma_z}{2\pi\tilde{a}} \int dx \eta(x) \sum_{r\alpha s} r\alpha \exp(-2irq_F x) \times \exp\{-ir(\theta_{\rho+} + s\theta_{\sigma+} + \alpha\theta_{\rho-} + \alpha s\theta_{\sigma-})\}, \quad (6)$$

$$\mathcal{H}_{imp}^2 = \frac{-i\sigma_y}{2\pi\tilde{a}} \int dx \sum_{rs} r \exp\{-ir(2q_F x + \theta_{\rho+} + s\theta_{\sigma+})\} \times [\xi(x) \exp\{-i(\phi_{\rho-} + s\phi_{\sigma-})\} + \text{H.c.}], \quad (7)$$

where $K_{\rho+} = (v_{\rho+}/v_0)^{-1} = 1/\sqrt{1+4\bar{V}(0)/(\pi v_0)}$ and $K_{j\delta} = v_{j\delta}/v_0 = 1$ for the others. The Pauli matrices seen in \mathcal{H}_{imp}^i are due to the product of Klein factors.

With the above phase Hamiltonian, I calculate the dynamical conductivity $\sigma(\omega)$, which is expressed by the memory function, $M(\omega)$, as follows:¹⁶

$$\sigma(\omega) = \frac{-i\chi(0)}{\omega + M(\omega)}, \quad (8)$$

$$M(\omega) = \frac{(\langle F; F \rangle_\omega - \langle F; F \rangle_{\omega=0})/\omega}{-\chi(0)}, \quad (9)$$

where $\langle A; A \rangle_\omega \equiv -i \int dx \int_0^\infty dt e^{(i\omega - \eta)t} \langle [A(x, t), A(0, 0)] \rangle$ with $\eta \rightarrow +0$, $\langle \dots \rangle$ denotes the thermal average with respect to \mathcal{H} , $F = [j, \mathcal{H}]$ with j being the current operator, and $\chi(0) = \langle j; j \rangle_{\omega=0}$. Since the present Hamiltonian conserves the total particle number, there are no nonlinear terms including $\phi_{\rho+}$. Then the current operator is expressed by $j = 2v_{\rho+}K_{\rho+}\partial_x\phi_{\rho+}/\pi$, which leads to $\chi(0) = -4v_{\rho+}K_{\rho+}/\pi$. To lowest order in D_1 and D_2 , $M(\omega)$ is calculated as

$$M(\omega) = \frac{2\pi v_{\rho+}K_{\rho+}}{\omega} \sum_{i=1,2} \frac{D_i}{(\pi\tilde{a})^2} \sin \frac{\pi K_i}{2} \left(\frac{2\pi T}{\omega_F} \right)^{K_i} \frac{1}{\pi T} \times \left\{ B\left(\frac{K_i}{2} - i\frac{\omega}{2\pi T}, 1 - K_i \right) - B\left(\frac{K_i}{2}, 1 - K_i \right) \right\}, \quad (10)$$

where $K_1 = (K_{\rho+} + K_{\sigma+} + K_{\rho-} + K_{\sigma-})/2$, $K_2 = (K_{\rho+} + K_{\sigma+} + K_{\rho-}^{-1} + K_{\sigma-}^{-1})/2$, ω_F is the cutoff energy given by v_0/\tilde{a} and $B(x, y) = \Gamma(x)\Gamma(y)/\Gamma(x+y)$ with $\Gamma(x)$ being the gamma function.

For $\omega \rightarrow 0$, $M(\omega)$ reduces to

$$M(0) = i2v_{\rho+}K_{\rho+} \sum_{i=1,2} \frac{D_i}{v_0^2} \left(\frac{2\pi T}{\omega_F} \right)^{K_i-2} \frac{\Gamma^2(K_i/2)}{\Gamma(K_i)}, \quad (11)$$

which leads to the resistivity,

$$\rho = \sigma(0)^{-1} = \frac{\pi^2}{2\tilde{a}} \sum_{i=1,2} \mathcal{D}_i \left(\frac{2\pi T}{\omega_F} \right)^{K_i-2} \frac{\Gamma^2(K_i/2)}{\Gamma(K_i)}, \quad (12)$$

where $\mathcal{D}_i = D_i\tilde{a}/(\pi v_0^2) = \tilde{a}/(\pi l_i)$ with $l_i = v_0\tau_i$ being the mean-free path. In the present case of $K_i = (K_{\rho+} + 3)/2$, the above expression results in $\rho = \rho_{B0}(2\pi T/\omega_F)^{(K_{\rho+}-1)/2} \Gamma^2((K_{\rho+}+3)/4)/\Gamma((K_{\rho+}+3)/2)$ where $\rho_{B0} = \pi/2(l_1^{-1} + l_2^{-1})$ is the resistivity for the noninteracting system in the Born approximation. It is remarkable that ρ/ρ_{B0} is

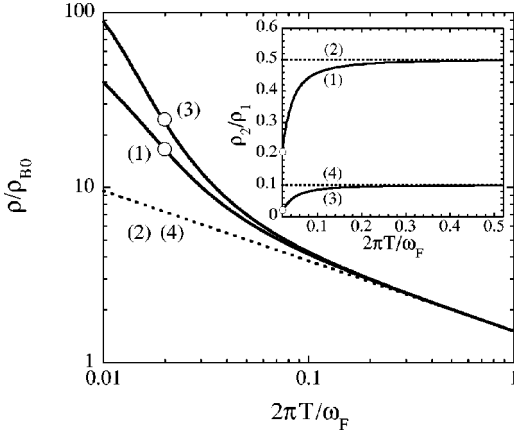


FIG. 1. Dependence on $2\pi T/\omega_F$ of the resistivity, ρ , normalized by ρ_{B0} , which is derived by the RG analysis for (1) $\mathcal{D}_1(0) = 1/300$ and $\mathcal{D}_2(0) = 1/600$ and (3) $\mathcal{D}_1(0) = 1/300$ and $\mathcal{D}_2(0) = 1/3000$. The dotted lines express the resistivity given by the perturbation theory for (2) $\mathcal{D}_1(0) = 1/300$ and $\mathcal{D}_2(0) = 1/600$ and (4) $\mathcal{D}_1(0) = 1/300$ and $\mathcal{D}_2(0) = 1/3000$. Here, $K_{\rho+} = 0.2$ is used and the white circle shows the temperature corresponding to $\mathcal{D}_1 \approx 1$, below which the perturbative RG analysis breaks down. Inset: The ratio, ρ_2/ρ_1 as a function of $2\pi T/\omega_F$. The numbers, (1)-(4), express the same cases as the main figure.

independent of the scattering strength. For typical nanotubes with $K_{\rho+} \approx 0.2$, the resistivity is enhanced compared to that without the Coulomb interaction and shows a temperature dependence as $\rho \propto T^{(K_{\rho+}-1)/2} \approx T^{-0.4}$.¹⁷ In the presence of the long-range Coulomb interaction, the phase expressing the symmetric charge fluctuation, $\theta_{\rho+}$, becomes rigid compared to the noninteracting case, which is expressed by the fact of $K_{\rho+}$ less than unity. Such a rigid phase is easily pinned by the impurity potential. Thus, the long-range Coulomb interaction enhances the resistivity. From the asymptotic behavior of Eq. (10) for $\omega \gg T$, the optical conductivity for high frequencies is calculated as $\sigma(\omega) \propto \omega^{(K_{\rho+}-5)/2} \sim \omega^{-2.4}$, which decays faster than that for the noninteracting case, $\sigma(\omega) \propto \omega^{-2}$. I note that the above two results of the resistivity and the optical conductivity do not depend on the filling, q_F . The umklapp scattering has been known to be another origin of resistivity. The umklapp scattering leads to $\rho \propto T^{(2K_{\rho+}-1)} \approx T^{-0.6}$,^{8,9} for $T \gg v_0 q_F$ and $\sigma(\omega) \propto \omega^{(2K_{\rho+}-3)} \approx \omega^{-2.6}$ for $\omega \gg v_0 q_F$. Though the powers due to the umklapp scattering are similar to those given by the impurity scattering, it is possible to separate them by tuning the gate voltage.

Next I take into account of the effects of localization by the renormalization-group (RG) method. Following Giamarchi and Schulz,¹⁸ averaging over the random fields, $\eta(x)$ and $\xi(x)$, I obtain the action, S_{imp} , corresponding to the impurity potential as follows:

$$S_{imp}^1 = -\frac{D_1}{2} \left(\frac{4}{\pi \tilde{a}} \right)^2 \int dx \int_0^\beta d\tau d\tau' \times \{ \cos(2q_F x + \theta_{\rho+}) \cos \theta_{\sigma+} \sin \theta_{\rho-} \cos \theta_{\sigma-} \\ \times \cos(2q_F x + \theta'_{\rho+}) \cos \theta'_{\sigma+} \sin \theta'_{\rho-} \cos \theta'_{\sigma-} \\ + \sin(2q_F x + \theta_{\rho+}) \sin \theta_{\sigma+} \cos \theta_{\rho-} \sin \theta_{\sigma-} \\$$

$$\times \sin(2q_F x + \theta'_{\rho+}) \sin \theta'_{\sigma+} \cos \theta'_{\rho-} \sin \theta'_{\sigma-} \\ - 2 \cos(2q_F x + \theta_{\rho+}) \cos \theta_{\sigma+} \sin \theta_{\rho-} \cos \theta_{\sigma-} \\ \times \sin(2q_F x + \theta'_{\rho+}) \sin \theta'_{\sigma+} \cos \theta'_{\rho-} \sin \theta'_{\sigma-} \}, \quad (13)$$

$$S_{imp}^2 = -D_2 \left(\frac{2}{\pi \tilde{a}} \right)^2 \int dx \int_0^\beta d\tau d\tau' e^{-i(\phi_{\rho-} - \phi'_{\sigma-})} \\ \times \{ \sin(2q_F x + \theta_{\rho+}) \cos \theta_{\sigma+} \cos \phi_{\sigma-} \\ \times \sin(2q_F x + \theta'_{\rho+}) \cos \theta'_{\sigma+} \cos \phi'_{\sigma-} \\ + \cos(2q_F x + \theta_{\rho+}) \sin \theta_{\sigma+} \sin \phi_{\sigma-} \\ \times \cos(2q_F x + \theta'_{\rho+}) \sin \theta'_{\sigma+} \sin \phi'_{\sigma-} \\ + i [\sin(2q_F x + \theta_{\rho+}) \cos \theta_{\sigma+} \cos \phi_{\sigma-} \\ \times \cos(2q_F x + \theta'_{\rho+}) \sin \theta'_{\sigma+} \sin \phi'_{\sigma-} \\ - \cos(2q_F x + \theta_{\rho+}) \sin \theta_{\sigma+} \sin \phi_{\sigma-} \\ \times \sin(2q_F x + \theta'_{\rho+}) \cos \theta'_{\sigma+} \cos \phi'_{\sigma-}] \}, \quad (14)$$

where $\theta_{j\delta} = \theta_{j\delta}(x, \tau)$, $\theta'_{j\delta} = \theta_{j\delta}(x, \tau')$, $\phi_{j\delta} = \phi_{j\delta}(x, \tau)$, and $\phi'_{j\delta} = \phi_{j\delta}(x, \tau')$. It should be noted that the interaction processes generated from the equal-time component in Eqs. (13) and (14) are disregarded. The results given in the following do not qualitatively changed even when the such processes are included because such operators are less divergent than S_{imp}^i . By calculating the various correlation functions to the lowest order of D_1 and D_2 , we have the following RG equations:

$$\mathcal{D}_1' = \{3 - (K_{\rho+} + K_{\sigma+} + K_{\rho-} + K_{\sigma-})/2\} \mathcal{D}_1, \quad (15)$$

$$\mathcal{D}_2' = \{3 - (K_{\rho+} + K_{\sigma+} + K_{\rho-}^{-1} + K_{\sigma-}^{-1})/2\} \mathcal{D}_2, \quad (16)$$

$$K_{j+}' = -(\mathcal{D}_1/X_1 + \mathcal{D}_2/X_2) K_{j+}^2 u_{j+}, \quad (17)$$

$$u_{j+}' = -(\mathcal{D}_1/X_1 + \mathcal{D}_2/X_2) K_{j+}^2 u_{j+}^2, \quad (18)$$

$$K_{j-}' = -(\mathcal{D}_1 K_{j-}^2/X_1 - \mathcal{D}_2/X_2) u_{j-}, \quad (19)$$

$$u_{j-}' = -(\mathcal{D}_1 K_{j-}/X_1 + \mathcal{D}_2 K_{j-}^{-1}/X_2) u_{j-}^2, \quad (20)$$

where $'$ denotes d/dl with $dl = d \ln(\tilde{a}'/\tilde{a})$ (\tilde{a}' is the new cutoff parameter), $X_1 = u_{\rho+}^{K_{\rho+}/2} u_{\sigma+}^{K_{\sigma+}/2} u_{\rho-}^{K_{\rho-}/2} u_{\sigma-}^{K_{\sigma-}/2}$, $X_2 = u_{\rho+}^{K_{\rho+}/2} u_{\sigma+}^{K_{\sigma+}/2} u_{\rho-}^{1/2K_{\rho-}} u_{\sigma-}^{1/2K_{\sigma-}}$, and $j = \rho$ or σ . The initial conditions for the above RG equations are as follows, $\mathcal{D}_i(0) = D_i \tilde{a}/(\pi v_0^2)$, $K_{\rho+}(0) = u_{\rho+}^{-1} = K_{\rho+}$, and $K_{\sigma+}(0) = K_{\rho-}(0) = K_{\sigma-}(0) = u_{\sigma+}(0) = u_{\rho-}(0) = u_{\sigma-}(0) = 1$. The above equations together with the initial conditions indicate that $K_{\rho-} = K_{\sigma-}$ and $u_{\rho-} = u_{\sigma-}$. In addition, the RG equations are invariant under the transformation, $\mathcal{D}_1 \leftrightarrow \mathcal{D}_2$ and $K_{j-} \leftrightarrow K_{j-}^{-1}$. Therefore, I can discuss the case of $\mathcal{D}_1(0) > \mathcal{D}_2(0)$ without loss of generality.

By solving the RG equations numerically and using Eq. (12), the resistivity is obtained as a function of temperature.¹⁹ I show the results for $\mathcal{D}_1(0) = 1/300$ and $\mathcal{D}_2(0) = 1/600$ and those for $\mathcal{D}_1(0) = 1/300$ and $\mathcal{D}_2(0) = 1/3000$ in Fig. 1. Surely, the resistivity is enhanced by the effects of the localization for low temperature. The inset

shows the ratio, ρ_2/ρ_1 , as a function of temperature, where ρ_1 (ρ_2) is the resistivity due to the intravalley (intervalley) scattering. In the present case where the intravalley scattering is stronger than the intervalley one, ρ_2/ρ_1 decreases with decreasing temperature. For the opposite case, ρ_1/ρ_2 decreases. The result is not obtained by the perturbation theory (dotted lines in the inset in Fig. 1), and then characteristic for the localized regime. It indicates that the two kinds of the backward scattering cannot coexist for this regime. As is seen in Eqs. (6) and (7), the intravalley (intervalley) scattering pins the phases, θ_{p+} , $\theta_{\sigma+}$, θ_{p-} , and $\theta_{\sigma-}$ (θ_{p+} , $\theta_{\sigma+}$, ϕ_{p-} , and $\phi_{\sigma-}$). Since the conjugate variables, θ_{p-} and ϕ_{p-} , or $\theta_{\sigma-}$ and $\phi_{\sigma-}$ cannot be pinned at the same time, the localization due to the two kinds of the scattering cannot happen simultaneously. In the present analysis, the quantitative discussion on the localized regime and crossover towards it have not been done. Therefore, more detailed investigation are needed for understanding of disordered SWNT's with the Coulomb interaction.

The above results of the metallic state with two valleys (2ν state) are compared to the transport properties of the metallic state with one valley (1ν state), which is realized by applying the parallel magnetic flux of $(i \pm 1/3)hc/e$ (i :integer) to the insulating tube.²⁰ In this case, the intervalley scattering is neglected. In addition, the exponent of the charge mode is given by $K_\rho = 1/\sqrt{1+2\bar{V}(0)/(\pi v_0)}$. Note that the difference in the coefficient of $\bar{V}(0)/(\pi v_0)$ between $K_{\rho+}$ and K_ρ results from that in the number of conducting bands. On the other hand, $K_\sigma = 1$. The resistivity ρ and the optical conductivity $\sigma(\omega)$ for high frequencies are, respectively, given by $\rho = \rho_{B0}^{1\nu} (2\pi T/\omega_F)^{K_\rho-1} \Gamma^2[(K_\rho+1)/2]/\Gamma(K_\rho+1)$ and $\sigma(\omega) \sim \omega^{K_\rho-3}$, with $\rho_{B0}^{1\nu} = \pi/l_1$ being the resistivity for the 1ν state by the Born approximation. Thus the behaviors in the 1ν state are different from those in the 2ν state. Since

$\Gamma^2[(K_\rho+1)/2]/\Gamma(K_\rho+1) > \Gamma^2[(K_{\rho+}+3)/4]/\Gamma[(K_{\rho+}+3)/2] > 1$ and $K_\rho - 1 < (K_{\rho+}-1)/2 < 0$ as a function of $\bar{V}(0)$, the effects of the Coulomb interaction are stronger in the 1ν state than in the 2ν state. From these results, it is expected that the resistivity (optical conductivity) of multiwall carbon nanotubes, in which both the metallic and insulating carbon nanotubes exist, shows different temperature (frequency) dependence in cases without parallel magnetic flux and with that of $hc/(3e)$.

In conclusion, I investigated the transport properties of the disordered SWNT's with Coulomb interaction. I found that the interaction enhances the resistivity, leads to a power-law dependence of the resistivity as a function of temperature, and modifies the power of the frequency of the optical conductivity. In addition, it is shown that the intravalley and the intervalley backward scattering cannot coexist in the localized regime. Differences between the 2ν and 1ν state were also discussed. For away from half-filling, the gaps induced by the Coulomb interaction, Δ , are given as $\Delta/\omega_F \sim e^{-c/u}$,^{7,8} with $u \sim a/(2\pi R)$ and $c \sim O(1)$, and thus very small for typical SWNT's. Therefore, the results obtained in this paper will be well observed for away from half filling with $T \ll v_0 q_F$ or $\omega \ll v_0 q_F$. The increase of the resistance with decreasing temperature observed in SWNT's (Ref. 21) may be due to the impurity scattering because the difference in the work function of the metallic electrode and the nanotube results in a downward shift of Fermi level of the nanotube by a few tenths of an eV.²²

The author would like to thank T. Ando, G. E. W. Bauer, Yu. V. Nazarov, A. A. Odintsov, Y. Tokura, A. Furusaki, H. Suzuura, and A. Khaetskii for stimulating discussions. This work was supported by a Grant-In-Aid for Scientific Research (11740196) from the Ministry of Education, Science, Sports and Culture, Japan.

¹A. Thess *et al.*, Science **273**, 483 (1996).

²T. Ando and T. Nakanishi, J. Phys. Soc. Jpn. **67**, 1704 (1998).

³T. Ando, T. Nakanishi, and R. Saito, J. Phys. Soc. Jpn. **67**, 2587 (1998).

⁴L. Balents and M. P. A. Fisher, Phys. Rev. B **55**, R11 973 (1997).

⁵Yu. A. Krotov, D.-H. Lee, and Steven G. Louie, Phys. Rev. Lett. **78**, 4245 (1997).

⁶Hsiu-Hau Lin, Phys. Rev. B **58**, 4963 (1998).

⁷R. Egger and A. O. Gogolin, Phys. Rev. Lett. **79**, 5082 (1997); Eur. Phys. J. B **3**, 281 (1998).

⁸C. Kane, L. Balents, and M. P. A. Fisher, Phys. Rev. Lett. **79**, 5086 (1997).

⁹H. Yoshioka and A. A. Odintsov, Phys. Rev. Lett. **82**, 374 (1999).

¹⁰A. A. Odintsov and H. Yoshioka, Phys. Rev. B **59**, R10 457 (1999).

¹¹S. J. Tans *et al.*, Nature (London) **394**, 761 (1998).

¹²M. Bockrath *et al.*, Nature (London) **397**, 598 (1999).

¹³Correspondence between the impurity potential of the present paper and those of Ref. 2 is as follows: $V_{\alpha\alpha}^+ = u_A$, $V_{\alpha-\alpha}^+ = u_A'$, $V_{\alpha\alpha}^- = u_B$, and $V_{\alpha-\alpha}^- = u_B'$.

¹⁴A. A. Abrikosov and I. A. Ryzhkin, Adv. Phys. **27**, 147 (1978).

¹⁵The cutoff parameter \bar{a} is considered to be of the order of the radius of the tube because only the lowest subbands are taken into account in the present discussion [T. Ando (private communication)].

¹⁶W. Götze and P. Wölfle, Phys. Rev. B **6**, 1126 (1972).

¹⁷The same exponent has been obtained in Refs. 7 and 8.

¹⁸T. Giamarchi and H. J. Schulz, Phys. Rev. B **37**, 325 (1988).

¹⁹T. Giamarchi, Phys. Rev. B **44**, 2905 (1991); **46**, 342 (1992).

²⁰H. Ajiki and T. Ando, J. Phys. Soc. Jpn. **62**, 1255 (1993); Physica B **201**, 349 (1994).

²¹C. L. Kane *et al.*, Europhys. Lett. **41**, 683 (1998).

²²J. W. G. Wildöer *et al.*, Nature (London) **391**, 59 (1998).